Stringent Null Constraint on Cosmological Evolution of the Proton-to-Electron Mass Ratio

Julian A. King and John K. Webb
School of Physics, University of New South Wales, Sydney, NSW, 2052, Australia

Michael T. Murphy
Centre for Astrophysics and Supercomputing, Swinburne University of Technology, Victoria, 3122, Australia

Robert F. Carswell
Institute of Astronomy, University of Cambridge, Cambridge CB3 0HA, United Kingdom
(Received 29 July 2008; published 19 December 2008)

We present a strong constraint on variation of the proton-to-electron mass ratio μ over cosmological time scales using molecular hydrogen transitions in optical quasar spectra. Using high quality spectra of quasars Q0405 − 443, Q0347 − 383, and Q0528 − 250, variation in μ relative to the present day value is limited to $\Delta\mu/\mu = (2.6 \pm 3.0) \times 10^{-6}$. We reduce systematic errors compared to previous works by substantially improving the spectral wavelength calibration method and by fitting absorption profiles to the forest of hydrogen Lyman α transitions surrounding each H_2 transition. Our results are consistent with no variation, and inconsistent with a previous $\approx 4\sigma$ detection of μ variation involving Q0405 − 443 and Q0347 − 383. If the results of this work and those suggesting that α may be varying are both correct, then this would tend to disfavor certain grand unification models.

DOI: 10.1103/PhysRevLett.101.251304 PACS numbers: 95.30.Dr, 14.20.Dh, 98.62.Ra, 98.80.Es

Searches have been undertaken in recent years for cosmological variations in fundamental, dimensionless constants. These searches are motivated by predictions of Kaluza-Klein theory, string theory, and other grand unification theories that the so-called ''fundamental constants'' may evolve over cosmological time scales. Although much of the focus has been on α, the fine structure constant, others have examined the proton-to-electron mass ratio, $\mu \equiv m_p/m_e$. The quantum chromodynamical scale, to which μ is sensitive, may vary faster than the quantum electrodynamical scale; hence, μ may vary more than α [1]. The wavelengths of the Lyman and Werner transitions of the H_2 molecule are sensitive to μ, and examination of H_2 absorption systems in quasar spectra allows one to search for any such variation, as was first noted by [2].

Attempts from 1995 to 2004 to detect a variation in μ yielded results statistically consistent with no change [3–11]. These searches (with the exception of [11]) were impaired by insufficiently accurate laboratory measurements of the H_2 wavelengths, as well as lower quality quasar spectra. Recent laboratory extreme ultraviolet (XUV) laser measurements [12,13] have yielded substantial improvements in H_2 wavelength accuracy.

Using these newly available wavelengths, Reinhold *et al.* [14] reanalyzed the observed H_2 wavelengths derived by Ivanchik *et al.* [11] from Very Large Telescope (VLT) spectra of absorbers associated with Q0405 − 443 (at redshift $z \approx 2.595$) and Q0347 − 383 (at $z \approx 3.025$), finding a change in μ of $\Delta\mu/\mu = (2.4 \pm 0.6) \times 10^{-5}$, where $\Delta\mu/\mu \equiv (\mu_z - \mu_0)/\mu_0$, μ_z is the measured value of μ at redshift z, and μ_0 is the present day laboratory value. However, it has since been demonstrated [15] that the techniques used to calibrate the wavelength scale of the Ultraviolet and Visual Echelle Spectrograph (UVES, on the VLT) produce both long- and short-range calibration errors [15]. These calibration errors directly impact the calculation of $\Delta\mu/\mu$. It is therefore important to reanalyze these spectra using the improved wavelength calibration techniques of [15], and we do so here. We also analyze an absorber towards Q0528 − 250 (at $z \approx 2.811$), which provides a new, strong constraint on $\Delta\mu/\mu$. We use the Voigt profile fitting program VPFIT to analyze our spectra.

For a given H_2 transition observed in an absorbing cloud at redshift $z_{\rm abs}$, the first-order shift in the wavelength λ_i compared to the laboratory wavelength λ_0 is given by

$$\lambda_i = \lambda_0(1 + z_{\rm abs})(1 + K_i\Delta\mu/\mu), \quad (1)$$

where K_i is the sensitivity coefficient associated with each transition, given by $K_i = (d\ln\lambda_i)/(d\ln\mu)$. $z_{\rm abs}$ is the redshift of the transitions measured provided that $\Delta\mu/\mu = 0$. If $\Delta\mu/\mu \neq 0$, $z_{\rm abs}$ corresponds to the redshift, determined from the ensemble of available transitions, of a transition with $K_i = 0$. Previous works have calculated K_i within a semiempirical framework [14,16]; Reinhold *et al.* [14] recently produced K_i coefficients of improved accuracy by including effects beyond the Born-Oppenheimer approximation. We use the K_i coefficients calculated by Reinhold *et al.* [14] and Ubachs *et al.* [16].

For a series of H_2 transitions, the best-fit value of $\Delta\mu/\mu$ may be determined in one of two ways. In the first, the ''reduced redshift method'' (RRM), one calculates an ob-

served redshift z_i for each transition, and then defines a reduced redshift

$$\zeta_i = \frac{z_i - z_{\rm abs}}{1 + z_{\rm abs}} = \frac{\Delta\mu}{\mu} K_i. \quad (2)$$

$\Delta\mu/\mu$ can then be determined by a linear fit to the observed ζ_i vs K_i distribution.

The second method (VPFIT method) involves fitting all available transitions simultaneously and solving for a single redshift for each identifiable absorbing H_2 component in the system. We refer to each fitted redshift as a velocity component because of the close proximity of these components in velocity space. $\Delta\mu/\mu$ is estimated by perturbing the laboratory H_2 wavelengths as $\lambda_0 \rightarrow \lambda_0[1 + K_i(\Delta\mu/\mu)]$ and minimizing χ^2 for the spectral data fitted. The value of $\Delta\mu/\mu$ at the minimum χ^2 is the best-fit value.

Although the VPFIT method has previously [6] been used to construct χ^2 vs $\Delta\mu/\mu$ curves, from which the best value of $\Delta\mu/\mu$ can be estimated, we instead include $\Delta\mu/\mu$ as a free parameter in the fit (within VPFIT), to be solved for concomitantly with the other line parameters; this yields a substantial improvement in computational speed and robustness.

The RRM has been used in most previous measurements and was the method used by [14]. This method is appealing because the required numerical methods are relatively simple. However, the VPFIT method is preferable in that fewer parameters are required to fit the data. In particular, the VPFIT method has $n_v(n_t - 1)$ fewer free parameters, where n_v is the number of velocity components and n_t is the number of transitions used. For Q0405 − 443 the VPFIT method yields 51 fewer parameters, for Q0347 − 373 it yields 67 fewer parameters, and for Q0528 − 250 it yields 252 fewer parameters.

It should be noted that the VPFIT method also improves the stability of the fitting process. In systems with multiple velocity components, particular transitions may have very poorly constrained line parameters, despite the fact that the best-fit line parameters may be well constrained over many transitions. In the RRM, this can cause the fitting algorithm to reject certain velocity components in some transitions, rendering those transitions unsuitable for inclusion in the fit. Using the VPFIT method, the reduction in the number of free parameters as a result of requiring each velocity component to occur at a single redshift helps to stabilize the fit, allowing for the inclusion of a greater number of transitions.

Each of the molecular hydrogen transitions involved falls within the Lyman α forest, a dense series of absorption lines blueward of the hydrogen Lyman α emission line of the quasar. These transitions substantially complicate the analysis; the narrow molecular hydrogen absorption lines are often situated deep within much broader, and usually complex, Lyman α lines. These contaminating atomic Lyman α transitions are insensitive to a change in μ. In contrast to previous works, we fit absorption profiles to all of the Lyman α transitions in the vicinity of each H_2 transition. This allows the inclusion of a greater number of H_2 transitions which would otherwise be excluded from the fit.

We have reduced the total number of free parameters in the fit by tying together physically linked parameters. In particular, we tie the Doppler (linewidth) parameters together for H_2 transitions with the same rotational quantum number J of the initial state. For the transitions we have analyzed, $J \in [0, 4]$. Each error estimate is multiplied by $\sqrt{\chi^2_\nu}$ (where χ^2_ν is the χ^2 per degree of freedom for the whole fit), to account for a nonideal fit.

Our inclusion of the Lyman α forest within the fitting process increases the number of free parameters in the fit substantially (to over 1000 in each quasar spectrum). With such a large parameter space, convergence of the optimization algorithm must be checked. References [17,18] demonstrated that the results of [19–22] (in relation to α) were flawed in this respect. Our algorithm demonstrates the proper convergence, in that $\Delta\mu/\mu$ vs χ^2 curves possess the correct parabolic shape, with derived 1σ error bounds on $\Delta\mu/\mu$ that agree with those produced by VPFIT.

The system toward Q0347 − 373 contains a single H_2 velocity component. The system towards Q0405 − 443 has a second velocity component, separated by ≈ 13 km s^{-1} in velocity space [14]. However, many of its transitions are weak or are heavily blended, and so we have not utilized the second component here.

The H_2 system towards Q0528 − 250 is more complicated. Previous attempts to examine this system have yielded varied and comparatively poor results [6,10] because the spectra used had substantially lower signal-to-noise ratio than those currently available from VLT. Ledoux *et al.* [23] report the detection of multiple velocity components in the Q0528 − 250 system (that is, multiple systems separated in velocity space), and Srianand *et al.* [24] model the absorber with two components.

We have tried modeling the absorber towards Q0528 − 250 with 2, 3, and 4 velocity components. Two velocity components are plainly obvious as a substantial asymmetry in every line. Using the F test, the probability that the reduction in χ^2 from using three components instead of two is due to chance is $p = 4 \times 10^{-18}$. That is, a three component model is very strongly preferred to a two component model.

Comparing a model with four velocity components to a model with three gives $p = 1.8 \times 10^{-8}$. That is, the four component model is preferred over both the two and three component models. The use of a five component model produces a fit that is highly unstable numerically, and so we use the four component model as the fiducial model.

In modeling the multiple velocity components, we require that the ratio of the column densities between each velocity component is the same for transitions with the same quantum number J. Certain line parameters for the

TABLE I. Relative column densities and redshifts for the best four-component fit to Q0528 − 250, with 1σ uncertainties, derived from the $J = 1$ set of lines. The relative column density is the difference between the logarithm of the column density for each component and the logarithm of the column density for the strongest component. We use the $J = 1$ set of lines because they are the largest fraction of the data set.

Component	Relative column density (cm^{-2})	Redshift
1	0.00	2.811 003 6(24)
2	-0.10 ± 0.03	2.811 122 9(15)
3	-0.60 ± 0.10	2.810 933 4(37)
4	-1.89 ± 0.76	2.811 213 9(91)

four-parameter fit (with appropriate redshifts tied) are given in Table I.

Our results are set out in Tables II and III.

We resampled the ζ_i vs K_i graph with the bootstrap method [25], to check for consistency. That is, we generated 10^5 new data sets by randomly drawing data points, with replacement, from the original data set, such that each of the new data sets has the same number of points as the original data set. We then obtained the slope of the linear fit to each of these data sets, giving $\Delta\mu/\mu$ for each set; the mean of this ensemble should be consistent with the generating data. For each absorber, we found consistency between the bootstrap method, the VPFIT method, and the RRM.

The RRM is not appropriate for Q0528 − 250 because the line parameters for each of the velocity components within a given transition are strongly correlated. So, for Q0528 − 250, groups of 4 points in a ζ_i vs K_i plot (the RRM method) are not independent. Thus the RRM method breaks down, as it uses linear least-squares fitting, which requires independence of all the data points. This demonstrates the superiority of the VPFIT method over the RRM. These correlations are correctly incorporated into the VPFIT method, as $\Delta\mu/\mu$ is determined from χ^2 on the total model.

We checked that using 4 velocity components (instead of 2 or 3) has no significant effect on the result by solving for $\Delta\mu/\mu$ (within VPFIT), with 2 and 3 velocity component models. This produces $\Delta\mu/\mu = (-0.6 \pm 3.8) \times 10^{-6}$ and $\Delta\mu/\mu = (-1.4 \pm 3.8) \times 10^{-6}$, respectively. These are similar to each other and to the result for the four velocity component model. This demonstrates the insensitivity of the result to having used the statistically preferred velocity structure.

Combining the three measurements of $\Delta\mu/\mu$ obtained within VPFIT using a weighted mean yields the value $\Delta\mu/\mu = (2.6 \pm 3.0) \times 10^{-6}$. This is null at a 1σ confidence level. This is our main result from a combined analysis of all three quasar absorbers.

For comparison with Reinhold *et al.* [14], a reduced redshift plot (Fig. 1) including only Q0405 − 443 and Q0347 − 373 produces the result $\Delta\mu/\mu = (8.5 \pm 5.7) \times 10^{-6}$ (weighted fit) and $\Delta\mu/\mu = (7.9 \pm 8.1) \times 10^{-6}$ (unweighted fit). We also attempt to compare with [14] by including in the fit only those transitions used in that Letter. For Q0405 − 443, this removes 16 transitions and adds 3, the latter of which appear to be contaminated and were excluded from our main analysis. This yields, from the RRM, a Q0405 − 443 result of $\Delta\mu/\mu = (10.2 \pm 8.9) \times 10^{-6}$. This is offset from the result of $(27.8 \pm 8.8) \times 10^{-6}$ in [14]. For Q0347 − 373, we remove 35 transitions that are not used in [14], and include 4 which appear to be contaminated, to give a result of $\Delta\mu/\mu = (12.0 \pm 14.0) \times 10^{-6}$, compared with $(20.6 \pm 7.9) \times 10^{-6}$ from [14]. The weighted mean of our results in this circumstance is $\Delta\mu/\mu = (10.7 \pm 7.5) \times 10^{-6}$. It is difficult to make a direct statistical comparison, due to the fact that the spectra analyzed are not independent; however, in both cases we see a shift of $\Delta\mu/\mu$ towards 0. Although the inclusion of Q0528 − 250 clearly shifts the combined Q0405 − 443 + Q0347 − 373 result towards zero, our combined Q0405 − 443 + Q0347 − 373 result is null under all the circumstances considered.

More details regarding our results can be found in [26]. In particular, the reader may locate individual copies of our ζ_i vs K_i plots there, as well as some example spectra fits. Reference [26] does not contain any information important to our result that is not included here.

Our final result of $\Delta\mu/\mu = (2.6 \pm 3.0) \times 10^{-6}$ represents a significant increase in precision over previous works (a factor of ≈ 2). This result is entirely consistent with $\Delta\mu/\mu = 0$ over cosmological time scales. It is also consistent with the recently published work of Murphy *et al.* [27], who find that $\Delta\mu/\mu = (0.74 \pm 0.47_{\text{stat}} \pm 0.76_{\text{syst}}) \times 10^{-6}$ using the inversion transitions of ammonia. Note, however, that the ammonia constraint is at $z = 0.685$ while all our constraints are at $z > 2.5$; they may not be directly compared without a theory of cosmologically evolving μ.

TABLE II. Values of $\Delta\mu/\mu$ obtained using the VPFIT method, derived from each of the quasar spectra. n is the number of transitions (per velocity component, for Q0528 − 250). The weighted mean given here is our preferred result.

Quasar spectrum	$\Delta\mu/\mu$ (VPFIT)	χ^2_ν	z	n
Q0405 − 443	$(10.1 \pm 6.2) \times 10^{-6}$	1.42	2.595	52
Q0347 − 373	$(8.2 \pm 7.4) \times 10^{-6}$	1.28	3.025	68
Q0528 − 250	$(-1.4 \pm 3.9) \times 10^{-6}$	1.22	2.811	64
Weighted mean	$(2.6 \pm 3.0) \times 10^{-6}$	n/a	2.81	n/a

TABLE III. Values of $\Delta\mu/\mu$ using the RRM, derived from each of the quasar spectra. n is the number of transitions.

Quasar spectrum	$\Delta\mu/\mu$ (RRM)	χ^2_ν	z	n
Q0405 − 443	$(10.9 \pm 7.1) \times 10^{-6}$	1.01	2.595	52
Q0347 − 373	$(6.4 \pm 10.3) \times 10^{-6}$	1.13	3.025	68
Q0405 + Q0347	$(8.5 \pm 5.7) \times 10^{-6}$	1.06	2.810	120
Q0528 − 250	···	···	···	64

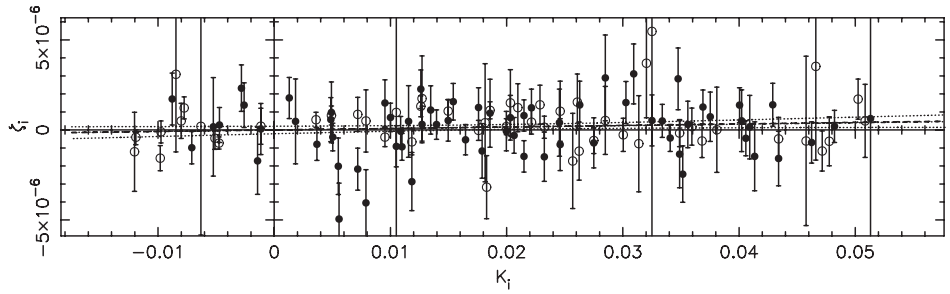

FIG. 1. Reduced redshift plot (ζ_i vs K_i) for Q0405 − 443 and Q0347 − 373 with gradient $\Delta\mu/\mu = (8.5 \pm 5.7) \times 10^{-6}$ (dashed line). Q0347 − 373 is represented by closed circles, and Q0405 − 443 is represented by open circles. The unweighted fit, a dot-dashed line, is obscured by the weighted fit. The dotted lines give the 1σ confidence limit on the regression line. Note that this is not our preferred result, because it does not include Q0528 − 250 in the fit. This graph may be compared directly with Fig. 2 of [14].

The unification of all interactions clearly requires that any cosmological variations in the various fundamental constants will be linked to each other. Grand unified theories typically predict $\Delta\mu/\mu \approx R\Delta\alpha/\alpha$ [28–30], where both the sign and magnitude of R are strongly model dependent. $|R| \approx 30$–40 emerges from many grand unified theory models [28–30]. Generally speaking, $|R| \gg 1$. The most reliable constraint on α variation at present is $\Delta\alpha/\alpha = (-5.7 \pm 1.0) \times 10^{-6}$ [31]; the works of [19–22] and others have been demonstrated to be unreliable [17,18]. Taking both this and our new null result at face value, any variation in μ is almost 2 orders of magnitude below that expected on the basis of the α-variation results. If both these results are correct, those grand unified models which predict $|R| \gg 1$ are disfavored.

We would like to acknowledge V. V. Flambaum, for advice and support in various stages of this work.

[1] V. V. Flambaum, D. B. Leinweber, A. W. Thomas, and R. D. Young, Phys. Rev. D **69**, 115006 (2004).
[2] R. I. Thompson, Astron. Lett. **16**, 3 (1975).
[3] D. Varshalovich and S. Levshakov, J. Exp. Theor. Phys. Lett. **58**, 237 (1993).
[4] L. L. Cowie and A. Songaila, Astrophys. J. **453**, 596 (1995).
[5] D. A. Varshalovich and A. Y. Potekhin, Space Sci. Rev. **74**, 259 (1995).
[6] A. Y. Potekhin, A. V. Ivanchik, D. A. Varshalovich, K. M. Lanzetta, J. A. Baldwin, G. M. Williger, and R. F. Carswell, Astrophys. J. **505**, 523 (1998).
[7] A. V. Ivanchik, E. Rodriguez, P. Petitjean, and D. A. Varshalovich, Astron. Lett. **28**, 423 (2002).
[8] A. Ivanchik, P. Petitjean, E. Rodriguez, and D. Varshalovich, Astrophys. Space Sci. **283**, 583 (2003).
[9] S. Levshakov, M. Dessauges-Zavadsky, S. D'Odorico, and P. Molaro, Mon. Not. R. Astron. Soc. **333**, 373 (2002).
[10] W. Ubachs and E. Reinhold, Phys. Rev. Lett. **92**, 101302 (2004).
[11] A. Ivanchik, P. Petitjean, D. Varshalovich, B. Aracil, R. Srianand, H. Chand, C. Ledoux, and P. Boisśe, Astron. Astrophys. **440**, 45 (2005).
[12] J. Philip, J. P. Sprengers, T. Pielage, C. A. de Lange, W. Ubachs, and E. Reinhold, Can. J. Chem. **82**, 713 (2004).
[13] U. Hollenstein, E. Reinhold, C. A. de Lange, and W. Ubachs, J. Phys. B **39**, L195 (2006).
[14] E. Reinhold, R. Buning, U. Hollenstein, A. Ivanchik, P. Petitjean, and W. Ubachs, Phys. Rev. Lett. **96**, 151101 (2006).
[15] M. T. Murphy, P. Tzanavaris, J. K. Webb, and C. Lovis, Mon. Not. R. Astron. Soc. **378**, 221 (2007).
[16] W. Ubachs, R. Buning, K. S. E. Eikema, and E. Reinhold, J. Mol. Spectrosc. **241**, 155 (2007).
[17] M. T. Murphy, J. K. Webb, and V. V. Flambaum, Phys. Rev. Lett. **99**, 239001 (2007).
[18] M. T. Murphy, J. K. Webb, and V. V. Flambaum, Mon. Not. R. Astron. Soc. **384**, 1053 (2008).
[19] R. Srianand, H. Chand, P. Petitjean, and B. Aracil, Phys. Rev. Lett. **92**, 121302 (2004).
[20] H. Chand, R. Srianand, P. Petitjean, and B. Aracil, Astron. Astrophys. **417**, 853 (2004).
[21] S. A. Levshakov, M. Centurión, P. Molaro, and S. D'Odorico, Astron. Astrophys. **434**, 827 (2005).
[22] S. A. Levshakov, M. Centurión, P. Molaro, S. D'Odorico, D. Reimers, R. Quast, and M. Pollmann, Astron. Astrophys. **449**, 879 (2006).
[23] C. Ledoux, P. Petitjean, and R. Srianand, Mon. Not. R. Astron. Soc. **346**, 209 (2003).
[24] R. Srianand, P. Petitjean, C. Ledoux, G. Ferland, and G. Shaw, Mon. Not. R. Astron. Soc. **362**, 549 (2005).
[25] W. Press, S. Teukolsky, W. Vetterling, and B. Flannery, *Numerical Recipes in C* (Cambridge University Press, New York, 1992), 2nd ed
[26] J. A. King, J. K. Webb, M. T. Murphy, and R. F. Carswell, arXiv:0807.4366.
[27] M. T. Murphy, V. V. Flambaum, S. Muller, and C. Henkel, Science **320**, 1611 (2008).
[28] X. Calmet and H. Fritzsch, Eur. Phys. J. C **24**, 639 (2002).
[29] X. Calmet, Phys. Lett. B **540**, 173 (2002).
[30] P. Langacker, G. Segrè, and M. J. Strassler, Phys. Lett. B **528**, 121 (2002).
[31] M. T. Murphy, J. K. Webb, and V. V. Flambaum, Mon. Not. R. Astron. Soc. **345**, 609 (2003).